ORIGINAL ARTICLE

Imaging Phenotyping Using Radiomics to Predict Micropapillary Pattern within Lung Adenocarcinoma

So Hee Song, MD,[a] Hyunjin Park, PhD,[b,c] Geewon Lee, MD,[d] Ho Yun Lee, MD, PhD,[a,*] Insuk Sohn, PhD,[e] Hye Seung Kim, MS,[e] Seung Hak Lee, MS,[f] Ji Yun Jeong, MD,[g] Jhingook Kim, MD,[h] Kyung Soo Lee, MD, PhD,[a] Young Mog Shim, MD[h]

[a]*Department of Radiology and Center for Imaging Science, Samsung Medical Center, Sungkyunkwan University School of Medicine, Seoul, Republic of Korea*
[b]*Center for Neuroscience Imaging Research, Institute for Basic Science, Suwon, Republic of Korea*
[c]*School of Electronic and Electrical Engineering, Sungkyunkwan University, Suwon, Republic of Korea*
[d]*Department of Radiology and Medical Research Institute, Pusan National University Hospital, Pusan National University School of Medicine, Busan, Republic of Korea*
[e]*Biostatistics and Clinical Epidemiology Center, Samsung Medical Center, Seoul, Republic of Korea*
[f]*Department of Electronic, Electrical and Computer Engineering, Sungkyunkwan University, Suwon, Republic of Korea*
[g]*Department of Pathology, Kyungpook National University Hospital, Kyungpook National University School of Medicine, Daegu, Republic of Korea*
[h]*Department of Thoracic and Cardiovascular Surgery, Samsung Medical Center, Sungkyunkwan University School of Medicine, Seoul, Republic of Korea*

Received 3 July 2016; revised 22 November 2016; accepted 24 November 2016
Available online - 3 December 2016

ABSTRACT

Introduction: Lung adenocarcinomas (ADCs) with a micropapillary pattern have been reported to have a poor prognosis. However, few studies have reported on the imaging-based identification of a micropapillary component, and all of them have been subjective studies dealing with qualitative computed tomography variables. We aimed to explore imaging phenotyping using a radiomics approach for predicting a micropapillary pattern within lung ADC.

Methods: We enrolled 339 patients who underwent complete resection for lung ADC. Histologic subtypes and grades of the ADC were classified. The amount of micropapillary component was determined. Clinical features and conventional imaging variables such as tumor disappearance rate and maximum standardized uptake value on positron emission tomography were assessed. Quantitative computed tomography analysis was performed on the basis of histogram, size and shape, Gray level co-occurrence matrix–based features, and intensity variance and size zone variance–based features.

Results: Higher tumor stage (OR = 3.270, 95% confidence interval [CI]: 1.483–7.212), intermediate grade (OR = 2.977, 95% CI: 1.066–8.316), lower value of the minimum of the whole pixel value (OR = 0.725, 95% CI: 0.527–0.98800), and lower value of the variance of the positive pixel value (OR = 0.961, 95% CI: 0.927–0.997) were identified as being predictive of a micropapillary component within lung ADC. On the other hand, maximum standardized uptake value and tumor disappearance rate were not significantly different in groups with a micropapillary pattern constituting at least 5% or less than 5% of the entire tumor.

Conclusion: A radiomics approach can be used to interrogate an entire tumor in a noninvasive manner. Combining imaging parameters with clinical features can provide added diagnostic value to identify the presence of a micropapillary component and thus, can influence proper treatment planning.

Keywords: Lung adenocarcinoma; Micropapillary; Computed tomography; Quantitative imaging; Radiomics

*Corresponding author.

Drs. Song, Park, and G. Lee equally contributed to this work.

Disclosure: The authors declare no conflict of interest.

Address for correspondence: Ho Yun Lee, Department of Radiology and Center for Imaging Science, Samsung Medical Center, Sungkyunkwan University School of Medicine, 81 Irwon-ro, Gangnam-gu, Seoul 06351, Republic of Korea. E-mail: hoyunlee96@gmail.com

ISSN: 1556-0864
http://dx.doi.org/10.1016/j.jtho.2016.11.2230

Introduction

Adenocarcinoma (ADC) is the most common histological subtype of lung cancer in most countries, accounting for almost half of all lung cancers.[1] Because remarkable heterogeneity exists in clinical, radiologic, molecular, and pathologic features among ADC cases, there remains a need for detailed classification and universally accepted criteria for ADC. Therefore, a classification was published in 2011 by the International Association for the Study of Lung Cancer, American Thoracic Society, and European Respiratory Society to support clinical practice, research investigation, and clinical trials.[2] In this revised classification, invasive lung ADCs were divided into the five subtypes lepidic, acinar, solid, papillary, and micropapillary patterns (MPs) primarily on the basis of histologic features.[2] The term *predominant* is appended to all categories of invasive ADC, as most of these tumors consist of mixtures of the histologic subtypes.

Those tumors classified as micropapillary as a predominant subtype have been reported to have a poor prognosis, with a tendency toward recurrence and metastasis.[3–5] Furthermore, even a small portion of MP, specifically, less than 5% of the entire tumor, has been reported to have a significant prognostic impact on survival.[6] This adverse prognostic effect of an MP can influence the treatment plan. Therefore, preoperative diagnosis of ADC with an MP is critical for appropriate surgical planning. However, preoperative histologic examination using biopsy is derived from only a portion of a generally heterogeneous tumor, so that the properties of the lesion cannot be completely represented. Although some investigations have characterized the morphologic characteristics of tumors on computed tomography (CT) images, these characteristics are described subjectively and qualitatively.[7,8] We conducted a study to find quantitative CT features allowing us to discriminate an MP by adopting a radiomics approach. *Radiomics* refers to the extraction and analysis of large amounts of advanced quantitative imaging features reflecting radiologic spatial distributions within a tumor, and it has been expected to provide descriptive and predictive models relating image features to tumor phenotypes.[9,10]

The purpose of our study was to explore imaging phenotyping using a radiomics approach for predicting an MP within lung ADC.

Material and Methods

Patients

The present retrospective study was approved by the institutional review board at Samsung Medical Center (institutional review board file number 2016-04-135), and informed consent was waived for reviewing patients' medical records. We enrolled 511 consecutive patients with lung ADC who underwent complete resection at our institution (Samsung Medical Center, Seoul, Republic of Korea) from July 2003 to January 2011. We excluded patients who had CT images acquired with an inadequate CT protocol for radiomics analysis ($n = 162$, CT slice thickness of 3 mm or more) to extract radiomics features in an optimal isotropic resolution. Ten additional patients were excluded on account of technically difficult analysis by the radiomics approach owing to very small tumor size. Specifically, scans with thick axial slices or very small tumors may have fewer than three sequential axial slices and may not contain three pixels in all 13 directional components, thus making it impossible to extract Gray level co-occurrence matrix (GLCM)-based features. Ultimately, a total of 339 patients were included in this study.

Imaging Acquisition

Helical CT images were all obtained with a 64-detector row CT scanner (LightSpeed VCT, GE Healthcare, Waukesha, WI). The CT image parameters were as follows: detector collimation, 1.25 or 0.625 mm; field of view, 36 cm; beam pitch, 1.375 to 1.500; beam width, 10 to 20 mm; gantry speed, 0.5 or 0.6 seconds per rotation; 120 kVp; 125 mA; reconstruction interval, 1 to 2.5 mm; and matrix, 512×512 mm. The helical acquisitions were reformatted into contiguous 2.5- to 3.5-mm axial sections overlapping by 1 to 1.5 mm on a standard workstation. CT scanning was obtained 90 seconds after the administration of contrast material (100 mL of iopamidol [Iomeron 300 (Bracco, Milan, Italy)]) at a rate of 1.5 mL/s using a power injector. This was followed by a 20-cm^3 saline flush at a rate of 1.5 mL/s.

Data Collection

Study data were collected from electronic medical records. Clinical characteristics were evaluated at the time of diagnostic work-up. Sex, age, smoking status, Union for International Cancer Control stage, and operation type were recorded. We also determined whether the patient had undergone adjuvant therapy.

Histologic Evaluation

Histologic subtypes and grades of the lung ADCs were classified according to the International Association for the Study of Lung Cancer/American Thoracic Society/European Respiratory Society multidisciplinary classification of lung ADC.[2] In addition, when the micropapillary component was less than 5% of the entire tumor, the pathologists further determined the amount of the micropapillary component at intervals of 1%. Tumors with the MP constituting less than 1% of the entire

tumor were defined as absent. Details about the histologic evaluation were described in our previous report.[6]

Image Analysis

Our personal computer–based in-house software program was used for lesion segmentation. All CT scans were obtained in the full inspiratory phase. For each tumor, regions of interest were delineated on the axial images to generate a volume of interest that included the entire tumor with a semiautomatic approach. Additional manual correction was performed to exclude bronchovascular bundles and ground glass opacity boundary by two radiologists (S.H.S, a senior resident, and G.W.L, who had 10 years of experience in chest CT imaging). After a nodule had been segmented, radiomics features were calculated and extracted automatically. This quantitative CT analysis was performed by using histogram-based, size- and shape-based, GLCM-based, and intensity variance and size zone variance–based features (Fig. 1). Detailed information about textural features is included in Supplementary Tables 1 and 2.

The tumor disappearance rate (TDR) was calculated as follows: [1 – (Tumor area of the mediastinal windows/Tumor area of the lung windows)] × 100.[11] As for fludeoxyglucose F18 positron emission tomography (PET) analysis, maximum standardized uptake value (SUV_{max}) was extracted from the primary tumor in the PET images for each patient. PET/CT scans were obtained in 288 patients.

Statistical Analyses

Comparison of the clinical and histologic characteristics of each subgroup was performed using one-way analysis of variance. Survival rate was estimated by the Kaplan-Meier method, and the log-rank test was applied to compare survival distribution between subgroups. Reliability and reproducibility of tumor segmentation and feature extraction was estimated by comparing the intraclass correlation coefficient (ICC) values between the two radiologists in 49 randomly selected patients. We selected statistically significant features from demographic and pathologic factors and selected the radiomics variable with the lowest p value from each radiomics category to remove redundancy within the radiomics information, as in Aerts et al.[12] For two groups, a multivariate logistic regression model with the

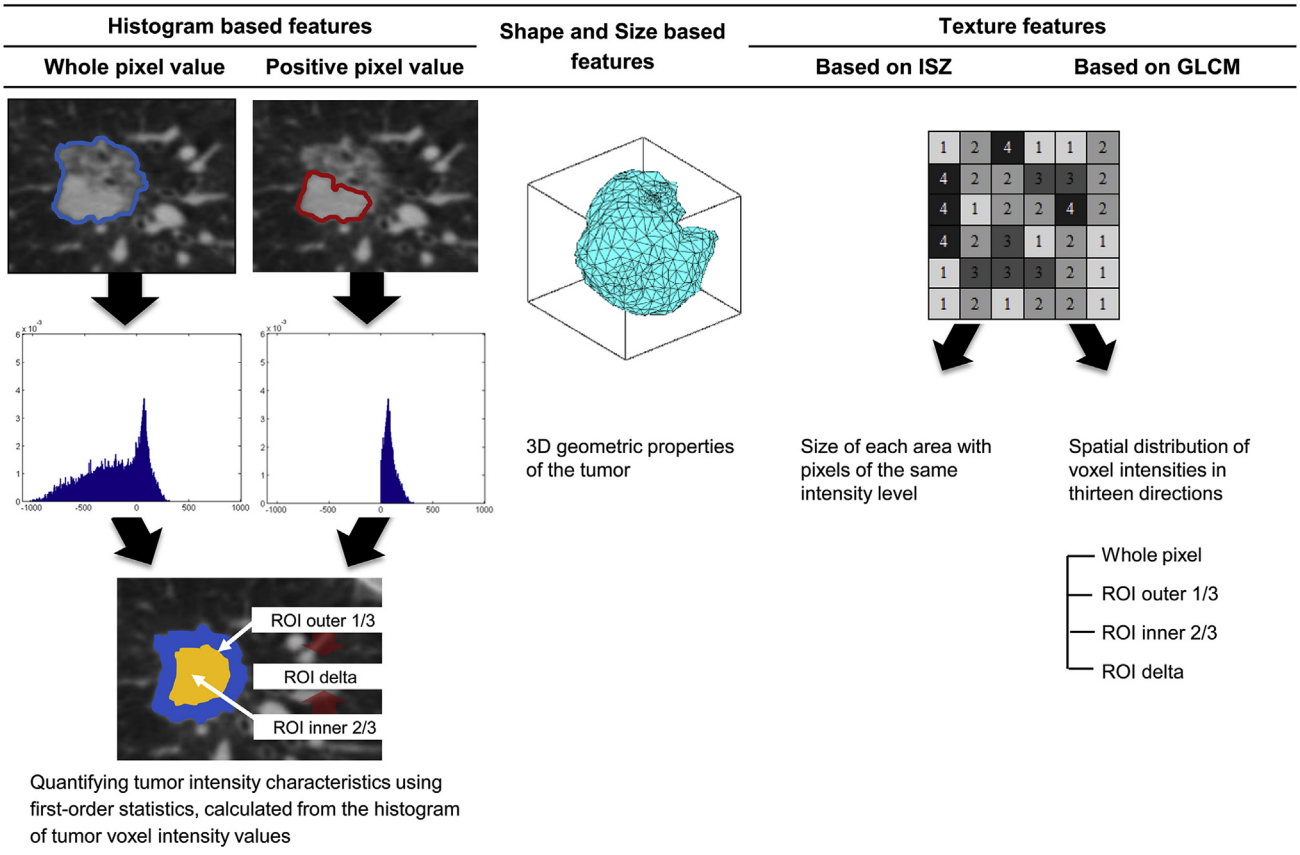

ISZ, Intensity variance and size zone variance value; GLCM, Gray-level co-occurrence matrix; ROI, Region of interest

Figure 1. Schematic illustration of quantitative computed tomography features. 3D, three-dimensional.

stepwise variable selection procedure based on Akaike's information criterion was applied to the selected features to fit the prediction model. For three groups, a multinomial logistic regression model with the stepwise variable selection procedure based on Akaike's information criterion was used to fit the prediction model. Tenfold cross-validation[13] was used to evaluate the performance of the prediction model. For two groups, a receiver operation characteristic curve was constructed and the area under the curve (AUC) was calculated. For three groups, multiclass AUC was calculated.[14] We also conducted decision curve analysis[15] to evaluate the clinical usefulness of the combination of radiomics features with clinical features by quantifying the net benefits at different threshold probabilities in the data set. The net benefit was calculated by using the following formula: Net benefit = True positive count/n – False positive count/n (Pt/1-Pt).[15] In this formula, true positive and false-positive counts are the numbers of patients with true positive and false-positive results and n is the total number of patients. The threshold probability Pt is the value at which the expected benefit of treatment is equal to the expected benefit of avoiding treatment. The decision curve was also plotted for the model of clinical feature only.

The model integrating radiomics and clinical features was further evaluated with respect to calibration by bootstrapping techniques: 1000 bootstrap samples were drawn, with replacement.[16] Calibration compares the predicted probability of an MP with its actual presence. A calibration graph was obtained by plotting the observed versus predicted probabilities. Thus, the ideal nomogram would show a localized regression plot that perfectly fits the 45-degree reference line when actual versus predicted probability is plotted.

Statistical analysis was executed using SAS software, version 9.4 (SAS Institute, Cary, NC) and R 3.2.5 (R Foundation for Statistical Computing, Vienna, Austria). p Values less than 0.05 indicated statistical significance.

Results

The patients were divided into two subgroups according to the amount of micropapillary component: (1) MP constituting at least 5% of the entire tumor (the MP $\geq$ 5% group) and (2) MP constituting less than 5% of the entire tumor (the MP $<$ 5% group). The clinical and histologic characteristics of patients are listed Supplementary Table 3. Of the 339 patients, 268 (79.1%) were in the MP $<$ 5% group, and the remaining 71 (20.9%) were in the MP $\geq$ 5% group. Between these two subgroups, there were no significant differences in sex, age, tumor size, SUV_{max}, and TDR value, whereas the difference in American Joint Committee on Cancer stage was statistically significant ($p = 0.048$). The MP $<$ 5% group tended to include patients with tumors at lower American Joint Committee on Cancer stages. Adjuvant therapy was performed significantly more often in the MP $\geq$ 5% group than in the MP $<$ 5% group ($p = 0.024$). Histologic grade was significantly different between the two subgroups ($p < 0.001$). Intermediate-grade tumors were most frequent in both groups. High-grade tumors were the second most common grade in the MP $<$ 5% group (29.5%), whereas the numbers of both low- and high-grade tumors were even in the MP $\geq$ 5% group. The distribution of predominant subtype was also different between the two groups ($p = 0.002$). Even though acinar subtype was most frequent in both subgroups (51.5% in MP $<$ 5% group and 52.1% in MP $\geq$ 5% group), the second most common subtypes were solid subtype in the MP $<$ 5% group (27.2%) and papillary subtype in the MP $\geq$ 5% group (21.1%). SUV_{max} and TDR were not significantly different between the two groups.

In addition, we classified the same patients into three more specifically defined subgroups: (1) MP constituting at least 5% of the entire tumor (the MP $\geq$ 5% group), (2) MP present but constituting less than 5% of the entire tumor (the 0 $<$ MP $<$ 5% group), and (3) absence ($<$ 1%) of the micropapillary subtype (the MP = 0 group). There were 191 patients (56.3%) in the MP = 0% group, 77 (22.7%) in the MP $<$ 5% group, and 77 (22.7%) in the MP $\geq$ 5% group. Clinical and histologic characteristics of these patients according to three groups are included in Supplementary Table 4.

Reliability and Reproducibility of Tumor Segmentation and Feature Extraction

The range of ICC values was 0.574 to 0.999, with mean a value of 0.857, representing a moderate or higher reliability level of agreement.

Prediction Model for the Presence of a Micropapillary Component within Lung Adenocarcinoma

In the two-group study, through categorical and stepwise selection, four features were ultimately identified as having the predictive ability for the presence of micropapillary component within lung ADC: two pathologic features that include stage and grade and two radiomics features that include the minimum of whole pixel values and variance of positive pixel value (Table 1). Overall, the MP-present group had a higher tumor stage (OR = 3.270, 95% confidence interval [CI]: 1.483–7.212), intermediate grade (OR = 2.977, 95% CI: 1.066–8.316), and lower value for the minimum of whole pixel values (OR = 0.725, 95% CI: 0.527–0.98800) and

Table 1. Prediction of the Presence of a Micropapillary Component or Presence of a Micropapillary Component Equal to or More Than 5% within Lung Adenocarcinoma

Prediction of presence of micropapillary component within lung adenocarcinoma

Selected Features	Reference	*p* Value	OR	95% CI
Smoking	Nonsmoking	0.032	2.859	1.095-7.467
UICC stage	Stage I	0.013	3.270	1.483-7.212
Histologic grade	Low grade	<0.001	2.977	1.066-8.316
Minimum of whole pixel values		0.048	0.725	0.527-0.988
Variance of positive pixel values		0.035	0.961	0.927-0.997

Prediction of presence of micropapillary component ≥5% within a lung adenocarcinoma

Selected features	Reference	*p* Value	OR	95% CI
Histologic grade	Low grade	<0.001	0.23	0.087-0.618
Sphericity value		0.0178	0.302	0.124-0.736
Difference entropy value at outer portion based on GLCM		0.0039	0.322	0.153-0.679

CI, confidence interval; UICC, Union for International Cancer Control; GLCM, Gray level co-occurrence matrix.

lower value for the variance of positive pixel values (OR = 0.961, 95% CI: 0.927–0.997). The sensitivity and specificity of categorical selection were 0.5493 and 0.6404, respectively, and those of stepwise selection were 0.8451 and 0.3558, respectively. The AUC of stepwise selection was 0.7511, as shown in Supplementary Figure 1.

As for the predictive ability of the MP ≥ 5% group, after the same process of selection, the following three features were identified: grade, sphericity value, and difference entropy value at outer portion based on GLCM (see Table 1). The AUC of stepwise selection was 0.6082.

Clinical Usefulness of the Prediction Model

The decision curve analysis for the model integrating radiomics features with clinical features and for the model using clinical features only is presented in Figure 2. The decision curve showed that if the threshold probability is greater than 20%, using the clinical features or a combination of clinical and radiomics features to predict MP adds more benefit than the treat-all-patients scheme or the treat-none scheme. In particular, the model integrating radiomics and clinical features gets more net benefit than the model using clinical features only at a threshold probability between 20% and 40%. Although this finding was reversed at a threshold probability greater than 40%, it can be meaningful because the reported incidence of MP is relatively low.

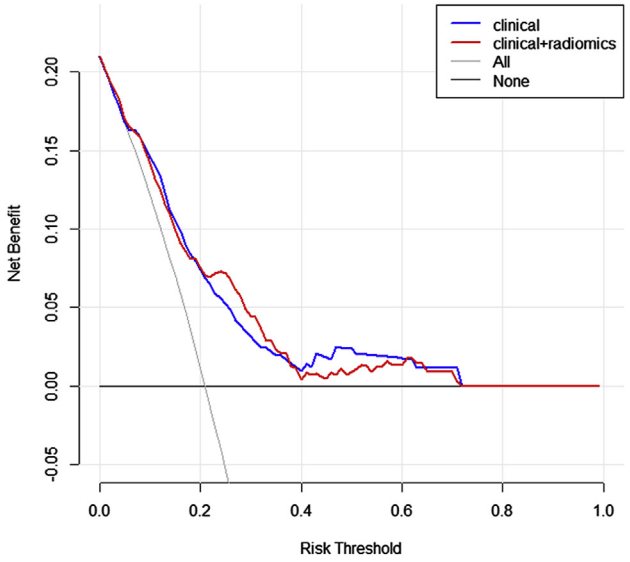

Figure 2. Decision curve analysis for the model using clinical features and the model with addition of radiomics features. The *y* axis measures the net benefit. The *x* axis shows the threshold probability. The red line represents the model combining radiomics and clinical features. The blue line represents the model using clinical features only. The thin gray line represents the assumption that all patients have lung adenocarcinoma with a micropapillary pattern. The black line represents the assumption that no patients have a micropapillary pattern.

In the calibration plot, the prediction model combining radiomics and clinical features demonstrated good calibration. The AUC was 0.751 ($p < 0.001$, 95% CI: 0.690–0.811) (Supplementary Fig. 2).

Survival Outcome

The median overall survival (OS) and disease-free survival (DFS) times of the entire study population were 4.7 and 3.8 years, respectively. The median OS and DFS times in the MP < 5% group were 4.7 and 3.9 years, respectively, whereas the respective times in the MP ≥ 5% group were 4.5 and 2.8 years. In terms of DFS, survival was significantly better in the MP < 5% group than in the MP ≥ 5% group. The hazard ratio (HR) for recurrence in the MP ≥ 5% group was 1.804 ($p = 0.00$, 95% CI: 1.235–2.634) in the two subgroup study. Likewise, the higher the proportion of MP present, the more recurrence developed in the three subgroups study. The HRs for recurrence in the MP < 5% and MP ≥ 5% groups were 1.556 and 2.064, respectively ($p = 0.001$) (Table 2).

The patterns of recurrence for two subgroups and three subgroups are presented in Table 3. Locoregional recurrence was significantly more frequent in the MP ≥ 5% group than in the MP < 5% group ($p = 0.002$).

In addition, as shown in Figure 3, there was a tendency for OS to be better in patients who had a lesser

Table 2. Survival Analysis according to the Difference in Proportion of the Micropapillary Component

	Two Subgroups		Three Subgroups		
Survival	MP $< 5\%$	MP $\geq 5\%$	MP $= 0$	$0 <$ MP $< 5\%$	MP $\geq 5\%$
Progression-free survival					
No. patients	268	71	191	77	71
No. events	92	38	60	32	38
HR		1.804		1.556	2.064
95% CI		1.235-2.634		1.010-2.395	1.372-3.104
p Value	0.002		0.001		
Overall survival					
No. events	40	17	29	11	17
HR		1.586		1.025	1.596
95% CI		0.899-2.799		0.512-2.054	0.877-2.907
p Value	0.108		0.275		

MP, micropapillary; HR, hazard ratio; CI, confidence interval.

extent of MP, although the difference was not statistically significant. The HR for death in the MP $\geq 5\%$ group was 1.586 in the two-subgroup study ($p = 0.108$), and the HRs for death in the MP $< 5\%$ and MP $\geq 5\%$ groups were 1.025 and 1.596, respectively, in the three-subgroup study ($p = 0.275$) (see Fig. 3).

Discussion

Recently, attention has been drawn to ADCs containing an MP in view of its association with poor prognosis, including a tendency toward recurrence and metastasis.[17,18] In our study, the MP $< 5\%$ group showed a tendency to have a lower TNM stage, whereas the MP $\geq 5\%$ group showed more frequent N2 disease. Yeh et al.[19] reported that the presence of an MP was an independent predictor of pathologic N2 disease. The MP is also known to be associated with a higher rate of lymphatic invasion[20,21] and visceral pleural invasion,[22] as well as with lymph node metastasis.[20–23] We ascertained that the prognosis was worse with an increase in the extent of the micropapillary portion of tumors. Even though patients in the MP $\geq 5\%$ group underwent more adjuvant therapy than those in the MP $< 5\%$ group, DFS was worse in the MP $\geq 5\%$ group in our study, indicating the necessity for more aggressive adjuvant therapy. Tsao et al.[24] reported that the micropapillary predominant and solid predominant patterns were predictive markers for the benefit of adjuvant chemotherapy in DFS and OS in patients with early-stage lung ADC. This aggressive behavior of ADC with an MP can also influence surgical planning. Nitadori et al.[25] reported that patients with tumors with a micropapillary component of 5% or greater treated with limited resection were at a higher risk for recurrence than similar patients treated with lobectomy, suggesting that limited resection may not be the optimal surgical approach for lung ADC with a MP. Therefore, preoperatively grasping the presence of MP within ADC is important for optimal surgical planning and advance selection of candidates for aggressive postoperative adjuvant therapy. It is also important to determine the presence of a MP even in inoperable lung ADC because a biopsy sample may not reflect all the characteristics of a generally heterogeneous tumor.

Until now, few studies have reported on the imaging-based identification of a micropapillary component.[7,26,27] However, these studies were all subjective studies dealing with qualitative CT variables. Even in cases of commonly used quantitative imaging values, interestingly enough, TDR and SUV_{max} were not different between the MP $< 5\%$ and MP $\geq 5\%$ groups in our study, although they are usually important prognostic imaging biomarkers.[8,28] Meanwhile, radiomics is an emerging field in which converging images with higher-dimensional

Table 3. Pattern of Recurrence according to the Difference in Proportion of the Micropapillary Pattern

	Two Subgroups				Three Subgroups				
Characteristics	MP $< 5\%$	MP $\geq 5\%$	Total	*p* Value	MP $= 0$	$0 <$ MP $< 5\%$	MP $\geq 5\%$	Total	*p* Value
No. patients	268	71	339		191	77	71	339	
Locoregional	20 (7.5)	14 (19.7)	34	0.002	13 (6.8)	7 (9.1)	14 (19.7)	34	0.008
Distant metastasis	78 (29.1)	28 (39.4)	106	0.095	50 (26.2)	28 (36.4)	28 (39.4)	106	0.066

Note: Data in parentheses are percentages of the total number in the corresponding subgroups.
MP, micropapillary.

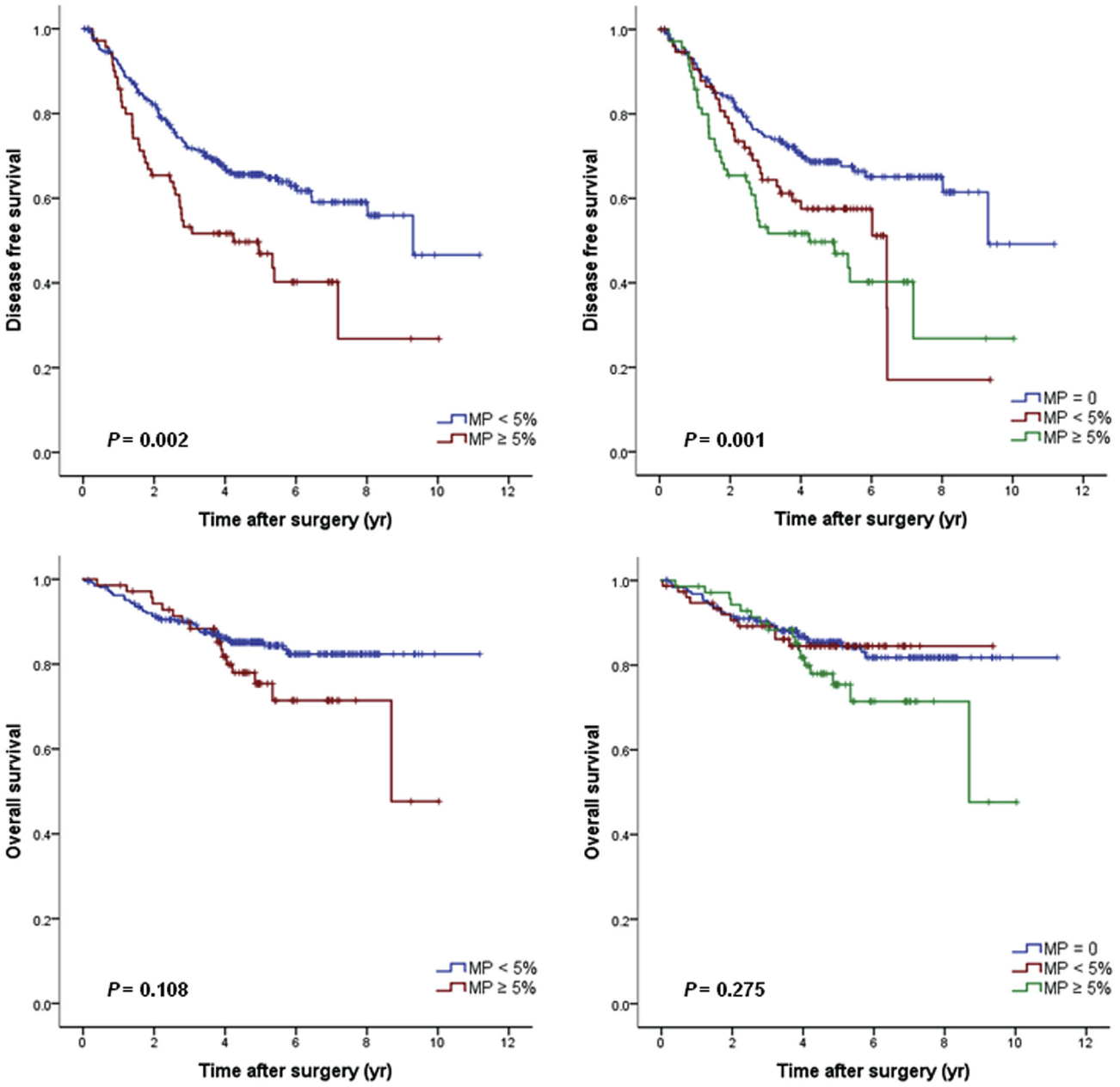

Figure 3. Disease-free survival and overall survival curves according to different proportions of micropapillary pattern.

data and subsequent mining of these data can improve decision support by providing comprehensive quantification of disease phenotypes.[29] In this study, we identified clinical and imaging findings for predicting an MP within a lung ADC. In addition to clinical features including smoking, TNM stage, and histologic grade, radiomics features such as the minimum of whole pixel values and variance of positive pixel value were selected as imaging predictors for the presence of a micropapillary component showing an OR less than 1. Two features were used to quantify tumor intensity characteristics using first-order statistics calculated from the histogram of all tumors or positive voxel intensity values, respectively. The feature minimum of whole pixel values enhances the areas of the tumor with ground glass opacity. Thus, we could interpret these results to mean that more solid, homogenous pixel-arranged tumors are associated with the micropapillary component. Sphericity value and difference entropy value at outer portion based on GLCM were also selected as predictors for the presence of micropapillary component equal to or more than 5% with an OR less than 1. Higher entropy means higher randomness of the histogram in interpretation of difference entropy value at outer portion based on GLCM. Thus, a homogenous pixel arrangement at the tumor periphery with a less

spherical shape could be associated with the micropapillary component. In particular, sphericity is a feature that describes how spherical the shape of the tumor is. Some investigators have reported that the MP usually exists at the peripheral area of the tumor.[30,31] Therefore, according to our results, the histological peripheral distribution of the MP may be reflected radiologically by the radiomics feature sphericity. Our results suggest possible value in combining clinical and imaging parameters for prediction of a micropapillary component beyond visual assessment.

Even allowing for intratumor heterogeneity, our result has greater clinical significance. Approximately 80% of ADCs show mixed subtype tumors, which is to say that a single most predominant subtype is not entirely representative of a large proportion of the tumors. In other words, the intermediate-grade ADC group according to the most predominant histologic subtype shows a very heterogeneous prognosis,[32] which means that information of the most predominant histologic subtype within the ADC is insufficient not only to predict prognosis but also to decide the appropriate management plan. Kadota et al.[32] found that tumors with intermediate-grade histologic features showing poor prognosis had either high-grade histologic features as the second predominant pattern or high mitotic count. However, the crux of the matter is that the MP, which is another poor prognostic indicator, tends to have a scattered, not clustered, distribution at the periphery or advancing edge of the tumor compared with at the center,[31] which is hard to discern with typical imaging. On the other hand, the radiomics approach shows local variation more sensitively with preservation of spatial heterogeneity.

Our study had several limitations. First, as is typical of retrospective studies from a single center, our study was limited by biases such as lack of random assignment, patient selection, and incomplete data acquisition. Further prospective investigation and, more importantly, a multicenter study are necessary. Second, the use of patients from a tertiary referral cancer institution may reflect a cohort with more aggressive disease. Third, external validation using an independent population was not performed. However, we conducted this study with a large number of patients and we attempted to perform tenfold cross-validation as a method of internal validation. In addition, a "rapid learning health care" approach would have provided a validation data set. In this era of an explosive amount of medical data, rapid learning health care is the organization of valuable routine clinical data that may be used in a broad range of areas from clinical care to research studies, and data infrastructure may provide a foundation for this system.[33–36] Overall, we believe that our result is meaningful in terms of building baseline research data for the next relevant study. Fourth, in terms of tumor segmentation, we used a semiautomated method with additional manual correction. Although our ICC values between two radiologists were good, a standardized scanning guideline seems necessary.[37]

In conclusion, the radiomics approach can be used to interrogate an entire tumor in a noninvasive manner, thus enabling the identification of imaging phenotypes to predict MP within a lung ADC. Tumors with a micropapillary component present have certain clinical and imaging features that can be used to differentiate them from other lung ADCs. The combination of imaging parameters with clinical features may provide added diagnostic value for the identification of presence of a micropapillary component and thus, can influence proper treatment planning such as candidate selection for aggressive postoperative adjuvant therapy.

Acknowledgments

This study was supported by a grant from the Korean Foundation for Cancer Research (KFCR-CB-2011-02-02).

Supplementary Data

Note: To access the supplementary material accompanying this article, visit the online version of the *Journal of Thoracic Oncology* at www.jto.org and at http://dx.doi.org/10.1016/j.jtho.2016.11.2230.

References

1. Matsuda T, Machii R. Morphological distribution of lung cancer from cancer incidence in five continents vol. X. *Jpn J Clin Oncol*. 2015;45:404.
2. Travis WD, Brambilla E, Noguchi M, et al. International Association for the Study of Lung Cancer/American Thoracic Society/European Respiratory Society international multidisciplinary classification of lung adenocarcinoma. *J Thorac Oncol*. 2011;6:244–285.
3. Sica G, Yoshizawa A, Sima CS, et al. A grading system of lung adenocarcinomas based on histologic pattern is predictive of disease recurrence in stage I tumors. *Am J Surg Pathol*. 2010;34:1155–1162.
4. Lee HY, Jeong JY, Lee KS, et al. Solitary pulmonary nodular lung adenocarcinoma: correlation of histopathologic scoring and patient survival with imaging biomarkers. *Radiology*. 2012;264:884–893.
5. Hoshi R, Tsuzuku M, Horai T, Ishikawa Y, Satoh Y. Micropapillary clusters in early-stage lung adenocarcinomas: a distinct cytologic sign of significantly poor prognosis. *Cancer*. 2004;102:81–86.
6. Lee G, Lee HY, Jeong JY, et al. Clinical impact of minimal micropapillary pattern in invasive lung adenocarcinoma: prognostic significance and survival outcomes. *Am J Surg Pathol*. 2015;39:660–666.
7. Lederlin M, Puderbach M, Muley T, et al. Correlation of radio- and histomorphological pattern of pulmonary adenocarcinoma. *Eur Respir J*. 2013;41:943–951.

8. Lee HY, Lee SW, Lee KS, et al. Role of CT and PET imaging in predicting tumor recurrence and survival in patients with lung adenocarcinoma: a comparison with the International Association for the Study of Lung Cancer/American Thoracic Society/European Respiratory Society classification of lung adenocarcinoma. *J Thorac Oncol*. 2015;10:1785–1794.
9. Lambin P, Rios-Velazquez E, Leijenaar R, et al. Radiomics: extracting more information from medical images using advanced feature analysis. *Eur J Cancer*. 2012;48:441–446.
10. Kumar V, Gu Y, Basu S, et al. Radiomics: the process and the challenges. *Magn Reson Imaging*. 2012;30:1234–1248.
11. Nakayama H, Yamada K, Saito H, et al. Sublobar resection for patients with peripheral small adenocarcinomas of the lung: surgical outcome is associated with features on computed tomographic imaging. *Ann Thorac Surg*. 2007;84:1675–1679.
12. Aerts HJ, Velazquez ER, Leijenaar RT, et al. Decoding tumour phenotype by noninvasive imaging using a quantitative radiomics approach. *Nat Commun*. 2014;5:4006.
13. Simon RM, Subramanian J, Li MC, Menezes S. Using cross-validation to evaluate predictive accuracy of survival risk classifiers based on high-dimensional data. *Brief Bioinform*. 2011;12:203–214.
14. Hand DJ, Till RJ. A simple generalisation of the area under the ROC curve for multiple class classification problems. *Machine Learning*. 2011;45:171–186.
15. Vickers AJ, Elkin EB. Decision curve analysis: a novel method for evaluating prediction models. *Med Decis Making*. 2006;26:565–574.
16. Efron B, Tibshirani RJ. *An Introduction to the Bootstrap*. Boca Raton, FL: CRC Press; 1994.
17. Hung JJ, Yeh YC, Jeng WJ, et al. Prognostic factors of survival after recurrence in patients with resected lung adenocarcinoma. *J Thorac Oncol*. 2015;10:1328–1336.
18. Cha MJ, Lee HY, Lee KS, et al. Micropapillary and solid subtypes of invasive lung adenocarcinoma: clinical predictors of histopathology and outcome. *J Thorac Cardiovasc Surg*. 2014;147:921–928.e922.
19. Yeh YC, Kadota K, Nitadori J, et al. International Association for the Study of Lung Cancer/American Thoracic Society/European Respiratory Society classification predicts occult lymph node metastasis in clinically mediastinal node-negative lung adenocarcinoma. *Eur J Cardiothorac Surg*. 2016;49:e9–e15.
20. Hung JJ, Yeh YC, Jeng WJ, et al. Predictive value of the International Association for the Study of Lung Cancer/American Thoracic Society/European Respiratory Society classification of lung adenocarcinoma in tumor recurrence and patient survival. *J Clin Oncol*. 2014;32:2357–2364.
21. Zhang J, Liang Z, Gao J, Luo Y, Liu T. Pulmonary adenocarcinoma with a micropapillary pattern: a clinicopathological, immunophenotypic and molecular analysis. *Histopathology*. 2011;59:1204–1214.
22. Miyoshi T, Satoh Y, Okumura S, et al. Early-stage lung adenocarcinomas with a micropapillary pattern, a distinct pathologic marker for a significantly poor prognosis. *Am J Surg Pathol*. 2003;27:101–109.
23. Amin MB, Tamboli P, Merchant SH, et al. Micropapillary component in lung adenocarcinoma: a distinctive histologic feature with possible prognostic significance. *Am J Surg Pathol*. 2002;26:358–364.
24. Tsao MS, Marguet S, Le Teuff G, et al. Subtype classification of lung adenocarcinoma predicts benefit from adjuvant chemotherapy in patients undergoing complete resection. *J Clin Oncol*. 2015;33:3439–3446.
25. Nitadori J, Bograd AJ, Kadota K, et al. Impact of micropapillary histologic subtype in selecting limited resection vs lobectomy for lung adenocarcinoma of 2 cm or smaller. *J Natl Cancer Inst*. 2013;105:1212–1220.
26. Mimae T, Miyata Y, Mimura T, et al. Radiologic findings to predict low-grade malignant tumour among clinical T1bN0 lung adenocarcinomas: lessons from histological subtypes. *Jpn J Clin Oncol*. 2015;45:767–773.
27. Ren J, Zhou J, Ding W, Zhong B, Zhou J. [Clinicopathological characteristics and imaging features of pulmonary adenocarcinoma with micropapillary pattern]. *Zhonghua Zhong Liu Za Zhi*. 2014;36:282–286 [in Chinese].
28. Berghmans T, Dusart M, Paesmans M, et al. Primary tumor standardized uptake value (SUVmax) measured on fluorodeoxyglucose positron emission tomography (FDG-PET) is of prognostic value for survival in non-small cell lung cancer (NSCLC): a systematic review and meta-analysis (MA) by the European Lung Cancer Working Party for the IASLC Lung Cancer Staging Project. *J Thorac Oncol*. 2008;3:6–12.
29. Gillies RJ, Kinahan PE, Hricak H. Radiomics: images are more than pictures, they are data. *Radiology*. 2016;278:563–577.
30. Chao L, Yi-Sheng H, Yu C, et al. Relevance of EGFR mutation with micropapillary pattern according to the novel IASLC/ATS/ERS lung adenocarcinoma classification and correlation with prognosis in Chinese patients. *Lung Cancer*. 2014;86:164–169.
31. Roh MS, Lee JI, Choi PJ, Hong YS. Relationship between micropapillary component and micrometastasis in the regional lymph nodes of patients with stage I lung adenocarcinoma. *Histopathology*. 2004;45:580–586.
32. Kadota K, Colovos C, Suzuki K, et al. FDG-PET SUVmax combined with IASLC/ATS/ERS histologic classification improves the prognostic stratification of patients with stage I lung adenocarcinoma. *Ann Surg Oncol*. 2012;19:3598–3605.
33. Abernethy AP, Etheredge LM, Ganz PA, et al. Rapid-learning system for cancer care. *J Clin Oncol*. 2010;28:4268–4274.
34. Schilsky RL, Michels DL, Kearbey AH, Yu PP, Hudis CA. Building a rapid learning health care system for oncology: the regulatory framework of CancerLinQ. *J Clin Oncol*. 2014;32:2373–2379.
35. Lambin P, Zindler J, Vanneste B, et al. Modern clinical research: how rapid learning health care and cohort multiple randomised clinical trials complement traditional evidence based medicine. *Acta Oncol*. 2015;54:1289–1300.
36. Bibault JE, Giraud P, Burgun A. Big Data and machine learning in radiation oncology: state of the art and future prospects. *Cancer Lett*. 2016;382:110–117.
37. Mackin D, Fave X, Zhang L, et al. Measuring computed tomography scanner variability of radiomics features. *Invest Radiol*. 2015;50:757–765.